Electronic Supplementary Material

A facile in-situ interfacial construction strategy of hierarchically distributed mixed-metal layered hydroxides/cellulose membrane towards efficient wastewater purification

Shuo Zhang,‡[a] Liping Shu,‡[b] Haohang Fang,[a] Weizhi Zhu,[a] Jianping Sun,[a] Fang Yang,[b] Yiqiang Wu,[c] Shaohong Shi*[a] and Fangchao Cheng*[a,c]

[a] State Key Laboratory of Featured Metal Materials and Life-cycle Safety for Composite Structures, School of Resources, Environment and Materials, Guangxi University, Nanning 530004, China

[b] Guangxi Key Laboratory of Natural Polymer Chemistry and Physics, College of Chemistry and Materials, Nanning Normal University, Nanning 530001, China

[c] College of Material Science and Engineering, Central South University of Forestry and Technology, Changsha 410004, China

‡ These authors contributed equally to this work.

* Email of corresponding author: shshichn@gxu.edu.cn; fangchaocheng@gxu.edu.cn

The Content of Supporting Information:

Total number of pages: 16

Total number of figures: 9

Total number of tables: 4

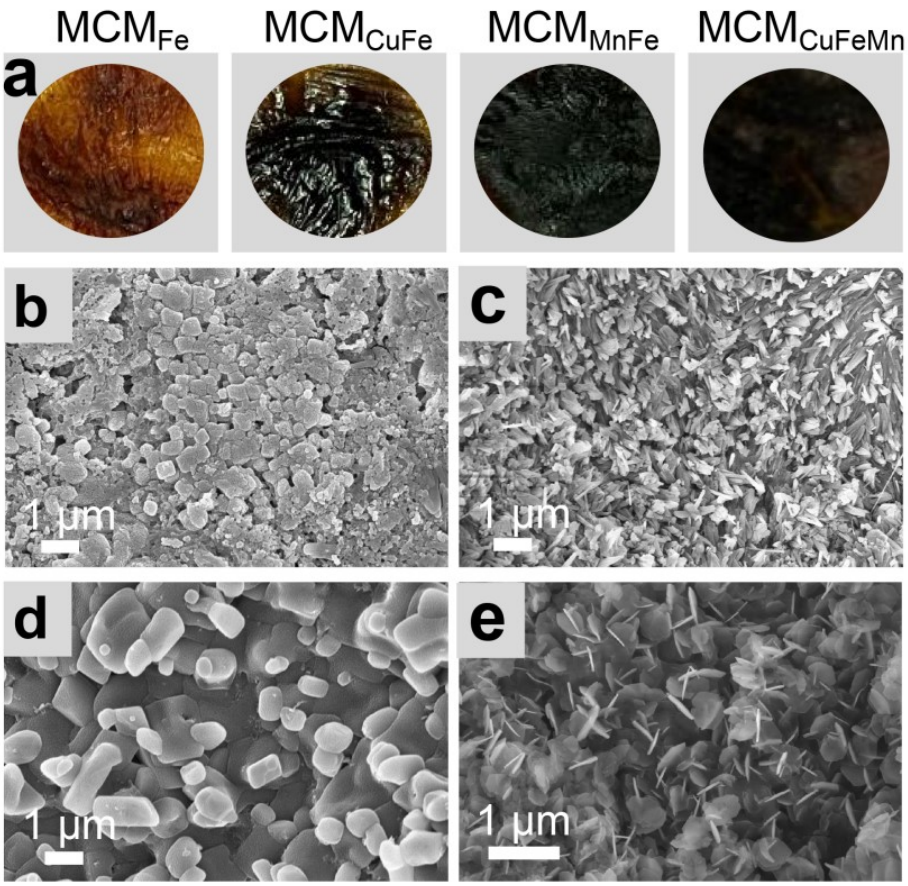

Fig. S1. The digital images of MCM_{Fe}、MCM_{CuFe}、MCM_{MnFe} and MCM_{CuFeMn} catalytic membranes (a); SEM images of MCM_{Fe} (b), MCM_{CuFe} (c), MCM_{MnFe} (d), and MCM_{CuFeMn} catalytic membranes (e).

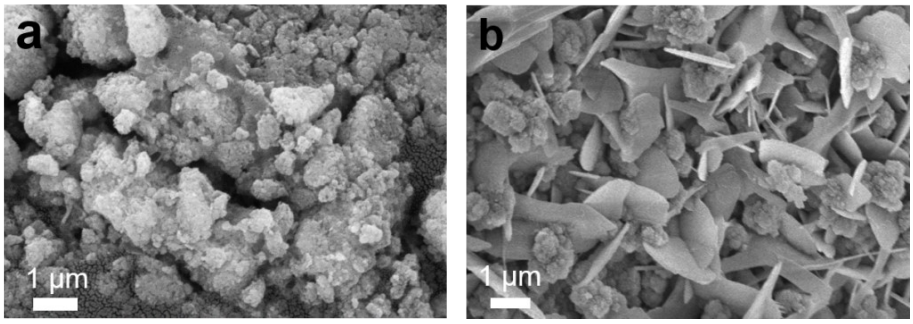

Fig. S2. SEM images of CuFeMn catalysts (a), and catalytic membrane with CuFeMn proportion of 9:3:9 (MCM_{939}) (b).

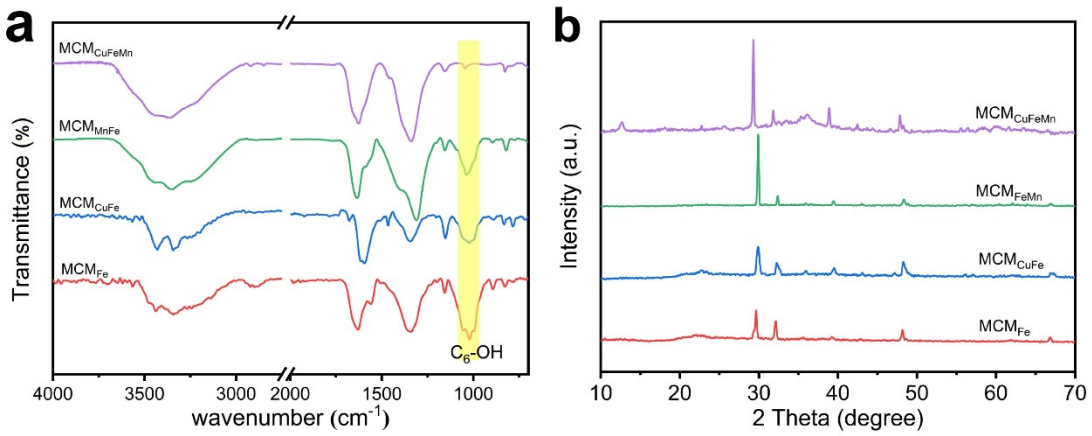

Fig. S3. The FT-IR spectra of MCM_{Fe}, MCM_{CuFe}, MCM_{MnFe} and MCM_{CuFeMn} catalytic membranes (a); The XRD patterns of MCM_{Fe}, MCM_{CuFe}, MCM_{MnFe} and MCM_{CuFeMn} catalytic membranes (b).

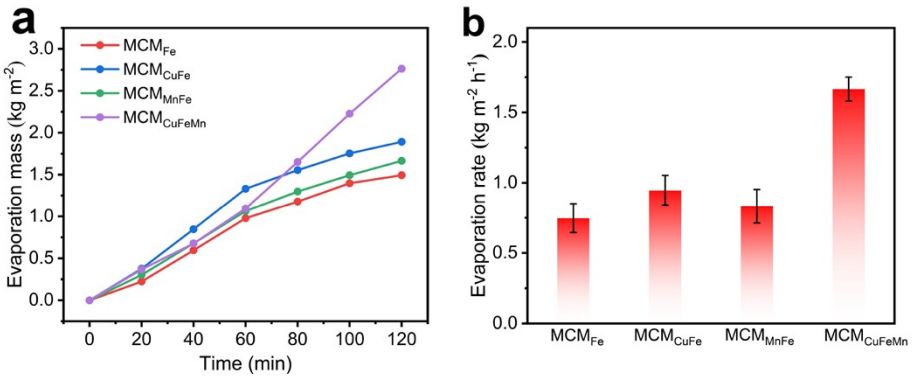

Fig. S4. Water evaporation mass (a) and evaporation rate of MCM_{Fe}, MCM_{CuFe}, MCM_{MnFe} and MCM_{CuFeMn} catalytic membranes (b).

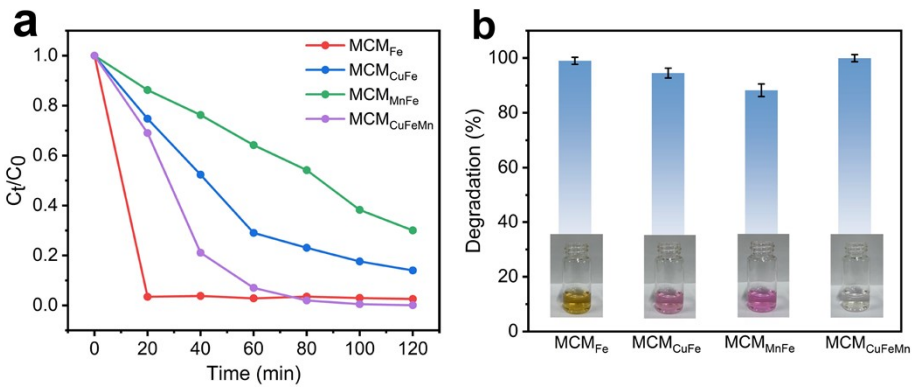

Fig. S5. The residual radios (C_t/C_0) (a) and the corresponding degradation efficiency of RhB after treatment with MCM_{Fe}, MCM_{CuFe}, MCM_{MnFe} and MCM_{CuFeMn} catalytic membranes (the inset showed the digital images of solution after photo-Fenton reaction) (b).

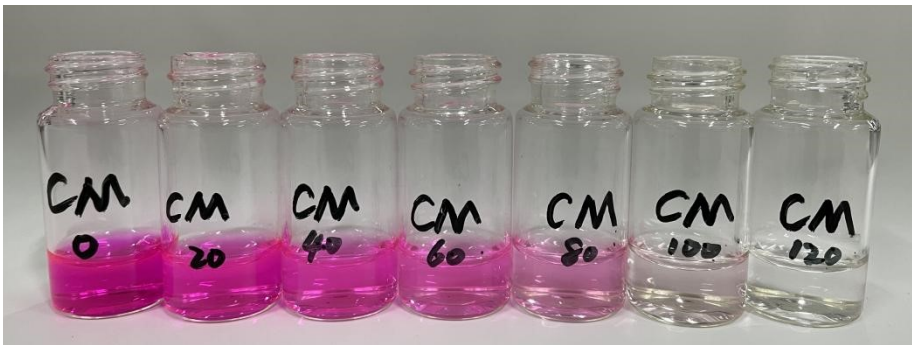

Fig. S6. Digital image of RhB solution after photo-Fenton reaction with MCM_{535} within 120 min.

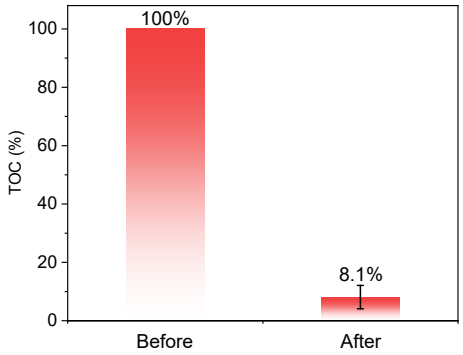

Fig. S7. The Total Organic Carbon (TOC) of MCM_{535} in 200 mg/L RhB solution before and after photo-Fenton reaction.

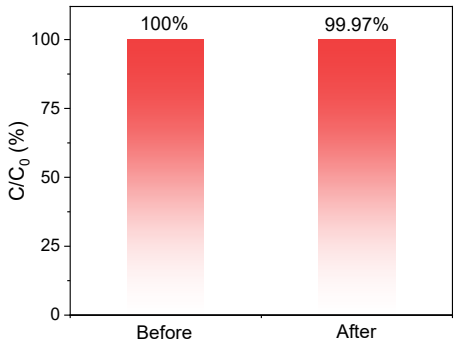

Fig. S8. The adsorption behavior of MCM_{535} in 200 mg/L RhB solution before and after a treatment of 30 minutes.

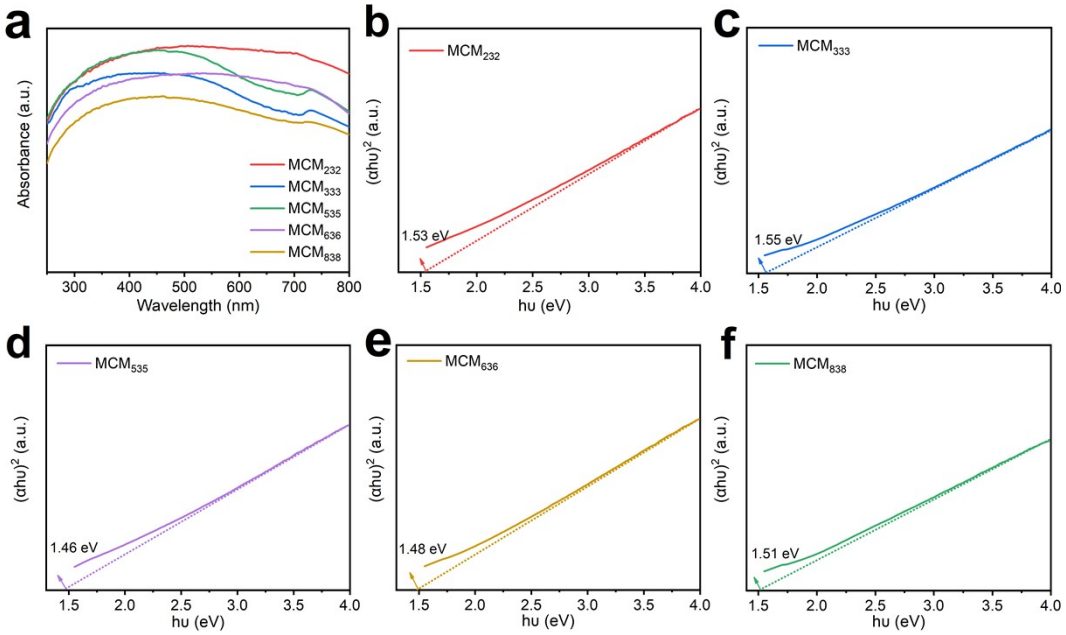

Fig. S9. Optical absorption spectra of catalytic membranes with different CuFeMn proportions (a); Estimated band-gap energy of MCM_{232} (b), MCM_{333} (c), MCM_{535} (d), MCM_{636} (e), and MCM_{838} catalytic membranes (f).

The UV-Vis diffuse reflectance spectra of MCM_{232}, MCM_{333}, MCM_{535}, MCM_{636}, and MCM_{838} were tested and converted into their absorption spectra according to the Kubelka Munk (K-M) method (Fig. S6a). The band gaps of different catalysts were determined by the following Equ. (1):

$$\alpha h\upsilon = A(h\upsilon - Eg)^{n} \quad (1)$$

Where, α, H, A, and Eg are light absorption coefficients, photon energy, proportional constants, and band-gap energy, respectively; N depends on the optical transition type of the semiconductor (n=1/2, direct absorption; n=2, indirect absorption). CuFeMn metal hydroxides are direct band gap semiconductors, so n=1/2, so the absorption band gap is determined by$(\alpha h\upsilon)^2$ and hυ. It can be calculated that the Eg estimates for MCM_{232}, MCM_{333}, MCM_{535}, MCM_{636}, and MCM_{838} were 1.53 eV, 1.55 eV, 1.46 eV, 1.48 eV, and 1.51 eV, respectively.

With the decrease of Eg, the less energy required for electronic transitions, and the stronger the photo-Fenton reaction activity. Therefore, MCM_{535} exhibited excellent photo-Fenton and water evaporation performance.

Tab. S1. Concentrations of Cu, Fe and Mn ions in the precursor solution

Molar ratio	Copper nitrate (mol/L)	Iron nitrate (mol/L)	Manganese nitrate (mol/L)
2:3:2	12.50	18.75	12.50
3:3:3	18.75	18.75	18.75
5:3:5	31.25	18.75	31.25
6:3:6	37.50	18.75	37.50
8:3:8	50.00	18.75	50.00
9:3:9	56.25	18.75	56.25

Tab. S2. Comparison of the evaporation rate and evaporation efficiency of our designed catalytic membrane with others previously reported in the literature.

Material	Light intensity (kW·m-2)	Evaporation rate ($kW \cdot m^{-2} \cdot h^{-1}$)	Evaporation efficiency (%)	Ref.
MCM_{535}	**1**	**1.58**	**90.4**	**This work**
MXene/cellulose	1	1.44	85.8	1
PVDF-HFP/PVA	1	1.02	72.0	2
Carbonaceous membrane	1	1.33	81.7	3
Ag/PANI	1	1.37	84.7	4
CNT/PI	1	1.26	72.7	5
rGO-CNT/PVDF	1	1.22	80.4	6
Fe_3O_4/carbon felt	1	1.32	85.0	7
Graphene/PPUS	1	1.31	85.3	8
Co-N-C/CF	1	1.88	87.0	9
CB-MHGM/PI	1	1.49	86.7	10
CB/PI	1	1.40	80.2	
MoS_2/Ti mesh	1	1.44	86.0	11
GTube membrane	1	1.44	77.0	12

Noted: PVDF-HFP: poly(vinylidene fluoride-co-hexafluoropropylene) nanofibers, PVA: polyvinyl alcohol, PAIN: polyaniline, CNT: carbon nanotube, PI: polyimide, rGO: reduced graphene oxide, PPUS: pyramid polyurethane sponge, Co-N-C: cobalt nanoparticles encapsulated in N-doped carbon framework, CF: carbon fiber, MHGM: modified hollow glass microspheres, CB: carbon black, and GTube: graphene tubes.

Tab. S3. The residual concentration of Cu, Fe and Mn ions in solution before and after photo-Fenton reaction.

	Initial concentration in MCM_{535} (mol/L)	Residual concentration in solution (mol/L)	
		before	after
Cu	12.50	3.59×10^{-6}	6.33×10^{-5}
Fe	18.75	4.69×10^{-6}	2.32×10^{-6}
Mn	12.50	4.51×10^{-6}	6.37×10^{-4}

Tab. S4. Comparison of the degradation capability of our designed catalytic membrane with others previously reported in the literature.

Material	Degradation efficiency (%)			Reacting time (min)	Ref.
	RhB	BPA	OTC		
MCM_{535}	**$100_{(200\ mg/L)}$**	**$89.7_{(40\ mg/L)}$**	**$90.9_{(40\ mg/L)}$**	**120**	**This work**
CdS/Fe_3O_4@NPC	$92.0_{(20\ mg/L)}$	-	-	75	13
$MoS_2/FeVO_4$	$90.0_{(10\ mg/L)}$	-	-	120	14
$LaFeO_3$/zeolites	$98.3_{(10\ mg/L)}$	-	-	90	15
α-FeOOH/BiOI	$100_{(20\ mg/L)}$			20	16
Mn@ peroxymonosulfate	-	$89.1_{(15\ mg/L)}$	-	60	17
Fe–O–Zr@MOF	-	$97.0_{(10\ mg/L)}$	-	30	18
PANI/MIL-88A(Fe)		$100_{(10\ mg/L)}$		60	19
MIL-88A		$100_{(10\ mg/L)}$		120	20
g-C_3N_4/FeOOH	-	-	$86.2_{(20\ mg/L)}$	120	21
Bi_2WO_6/CoAl-LDHs	-	-	$98.5_{(10\ mg/L)}$	60	22
OCN/$MnFe_2O_4$	-	-	$82.2_{(10\ mg/L)}$	60	23
$BiVO_4$	-	-	$83.0_{(10\ mg/L)}$	240	24

Noted: NPC: N-doped C, MOF: metal-organic framework, PANI: polyaniline, MIL-88A: Fe-based MOF, and CoAl-LDH: CoAl layered double hydroxide.

References

1. X. J. Zha, X. Zhao, J. H. Pu, L. S. Tang, K. Ke, R. Y. Bao, L. Bai, Z. Y. Liu, M. B. Yang and W. Yang, *ACS Appl. Mater. Interfaces.*, 2019, **11**, 36589-36597.
2. G. Xue, Q. Chen, S. Lin, J. Duan, P. Yang, K. Liu, J. Li and J. Zhou, *Glob. Chall.,* 2018, **2**, 1800001.
3. D. Wu, J. Liang, D. Zhang, C. Zhang and H. Zhu, *Sol. Energy Mat. Sol. C.*, 2020, 215, 110591.
4. R. Li, C. Zhou, L. Yang, J. Li, G. Zhang, J. Tian and W. Wu, *J. Hazard. Mater.* 2022, **424**, 127367.
5. X. Hou, R. Zhang and D. Fang, *Carbon*, 2022, 187, 310-320.
6. Y. Wang, C. Wang, X. Song, S. K. Megarajan and H. Jiang, *J. Mater. Chem. A*, 2018, **6**, 963-971.
7. Y. Geng, K. Zhang, K. Yang, P. Ying, L. Hu, J. Ding, J. Xue, W. Sun, K. Sun and M. Li, *Carbon*, 2019, **155**, 25-33.
8. Q. Yang, C. Xu, F. Wang, Z. Ling, Z. Zhang and X. Fang, *ACS Appl. Energy Mater.*, 2019, **2**, 7223-7232.
9. L. Cui, P. Wang, H. Che, X. Gao, J. Chen, B. Liu and Y. Ao, *Appl. Catal. B-Environ.*, 2023, **330**, 122556.
10. S. Wang, Y. Niu, L. Yan, W. Chan, Z. Zhu, H. Sun, J. Li, W. Liang and A. Li, *Compos. Sci. Technol.*, 2022, **228**, 109683.
11. Z. Chu, Z. Liu, Z. Li, Y. Cao, X. Tian, C. Jia, J. Wang, D. Wang, Z. Liu and W. Huang, *Mater. Today Sustain.*, 2022, **19**, 100223.
12. H. Yin, H. Xie, J. Liu, X. Zou and J. Liu, *Desalination*, 2021, **511**, 115116.
13. J. Zhang, L. Lin, B. Wang, Y. Zhang, Y. Wang, L. Zhang, Y. Jiang, H. Chen and M. Zhao, *Colloid. Surface. A.*, 2021, **625**, 126974.
14. Q. Liu, J. Zhao, Y. Wang, Y. Liu, J. Dong, J. Xia and H. Li, *Colloid. Surface. A.*, 2021, **623**, 126721.
15. T. T. N. Phan, A. N. Nikoloski, P. A. Bahri and D. Li, *J. Environ. Manage.*, 2019, **233**, 471-480.
16. Z.-H. Pan, Y. Wei, Q.-Y. Wang, K.-Y. Fan, J.-Y. Qi, S.-t. Wang and L.-Z. Zhang, *J. Environ. Chem. Eng.*, 2021, **9**, 106627.
17. Q. Si, W. Guo, B. Liu, H. Wang, S. Zheng, Q. Zhao, H. Luo, N. Ren and T. Yu, *Chem. Eng. J.*, 2022, **443**, 136399.
18. Z. Guan, S. Zhu, S. Ding, D. Xia and D. Li, *Chemosphere*, 2022, **299**, 134481.
19. D. D. Chen, X. H. Yi, L. Ling, C. C. Wang and P. Wang, *Appl. Organomet. Chem.*, 2020, **34**, 5795.
20. H. Fu, X.-X. Song, L. Wu, C. Zhao, P. Wang and C.-C. Wang, *Mater. Res. Bull.*, 2020, **125**, 110806.
21. W. Shi, W. Sun, Y. Liu, K. Zhang, H. Sun, X. Lin, Y. Hong and F. Guo, *J. Hazard. Mater.*, 2022, **436**, 129141.
22. B. Shao, Z. Liu, L. Tang, Q. Liang, Q. He, T. Wu, Y. Pan, M. Cheng, Y. Liu, X. Tan, J. Tang, H. Wang, H. Feng and S. Tong, *Chemosphere*, 2022, **291**, 133001.
23. H. Yi, C. Lai, X. Huo, L. Qin, Y. Fu, S. Liu, L. Li, M. Zhang, M. Chen and G. Zeng, *Environ. Sci-nano.*, 2022, **9**, 815-826.
24. T. Senasu, S. Youngme, K. Hemavibool and S. Nanan, *J. Solid. State. Chem.*, 2021, **297**, 122088.